

Sameera Samarakoon<sup>1</sup>

<sup>1</sup>Affiliation not available

February 9, 2023

**Phosphodiesterase- 5 (PDE5) Inhibitory Potential of  
Major Phytochemicals of *Withania somnifera* and  
*Cardiospermum halicacabum*: an *in silico* comparison with  
approved PDE5 inhibitors**

**Author Details:**

Irendra Wijewardana

Mishal Faizan

Dasuni Dilkini Eapasinghe

Kanishka S. Senathilake

Prasanna B. Galhena

Sameera R. Samarakoon

Kamani H. Tennekoon

Corresponding authors (Sameera Samarakoon and Kanishka Senathilake)

**Keywords:**

Rutin

Rutoside

Withaferin A

Withanolide

Ashwagandha

PDE-5 inhibitors

Molecular docking

*Withania somnifera*

Erectile dysfunction

*Cardiospermum halicacabum*

**Funding details:**

This work was funded by the Institute of Biochemistry, Molecular Biology and Biotechnology, University of Colombo.

**Data availability statement:**

All data produced during research are provided in the manuscript

## Abstract

The second messenger cyclic guanosine monophosphate (cGMP) produced in penile smooth muscle cells is responsible for triggering and maintain erection of penis. Phosphodiesterase type 5 (PDE5) is an enzyme that hydrolyses cGMP leading to penile flaccidity. Oral phosphodiesterase type 5 (PDE5) inhibitors such as sildenafil, tadalafil and avanafil remain the current standard for first-line treatment for erectile dysfunction (ED). *Withania somnifera* and *Cardiospermum halicacabum* are medicinal plants that are traditionally being used orally for the treatment of erectile dysfunction without any scientific evidence for their bioactivity. To validate these claims and to identify potential active ingredients, 53 major phytochemicals of *W. somnifera* and *C. halicacabum* were docked against the active site of the crystal structure of PDE5. Standard drugs sildenafil, tadalafil and avanafil were served as positive controls for molecular docking. Docked complexes with binding energies similar or greater than standard drugs were further studied by carrying out 100 ns molecular dynamics simulations and *in silico* adsorption, distribution, metabolism, excretion and toxicity (ADMET) predictions. Steroidal lactone withaferin A of *W. somnifera* was identified as potent inhibitor of PDE5 with predicted binding energy greater than that of sildenafil and avanafil while having very high oral bioavailability and less toxicity. Several other withaferin derivatives of *W. somnifera*, apigenin and rutine of *C. halicacabum* were also identified with less confident as potential PDE5 inhibitors. Overall results computationally validated the use of *Withania somnifera* for erectile dysfunction.

## **1. Introduction**

Cyclic guanosine monophosphate (cGMP) specific phosphodiesterase type 5 (PDE5) is a multidomain enzyme that functions as a dimer to hydrolyze cGMP thereby acting as a key modulator of cGMP signaling pathways in physiological processes such as smooth muscle relaxation and contraction (Rybalkin et al., 2003, Zhu & Strada, 2007, Tsai & Kass, 2009). PDE5 inhibitors were originally synthesized for treatment of hypertension and coronary heart disease. However due to high levels of PDE5 expression in the human corpus cavernosum compared to other tissues has made those inhibitors successful drugs against erectile dysfunction (Rotella, 2002). PDE5 inhibiting drugs such as sildenafil, vardenafil, tadalafil, and avanafil (Bischoff, 2004) have shown to increase penile blood flow and enhance endothelial function (Dhaliwal & Gupta, 2020). PDE5 inhibitors have also been successful in therapy of female sexual dysfunctions, premature ejaculation, radical prostatectomy, and Peyronie's disease (Gur et al., 2012, Andersson, 2018). Furthermore, it reduces tension and despondency (Soc  a et al., 2016).

PDE5 contains a N-terminal regulatory and dimerization GAF domain and a C terminal catalytic domain. GAF domain phosphorylation and substrate (cGMP) binding to non-catalytic allosteric site in the GAF domain increases the affinity of the PDE5 catalytic domain to cGMP (Turko et al., 1998, Corbin et al., 2000, Corbin, 2004). A c-terminal helical bundle of the catalytic domain adopts the substrate pocket which is composed of four sub sites, i.e. Q pocket (core pocket), M site (metal-binding site), H pocket (hydrophobic pocket) and L region (lid region). The Q pocket is a highly conserved region accommodating the

guanidine group of cGMP and includes the highly conserved Gln817, Phe820, Val782 and Tyr612 amino acid residues (Turko et al., 1999, Ahmed et al., 2021). Gln817 of the Q pocket forms hydrogen bonds with the guanine group of cGMP while other residues in Q pocket form hydrophobic interaction with cGMP. Importantly, the invariant Gln817 residue is the key substrate selectivity determinant in PDEs, which could hydrolyze either cGMP or cAMP which is controlled by surrounding residues that position the Gln817 in a specific orientation, depending on the nature of the PDEs (Soderling & Beavo, 2000). In PDE5, this is achieved by immobilization of the side chain amide group of Gln817 through a network of hydrogen bonds involving Gln817, Gln775, Gln775, Ala767 and Trp853 (Ahmed et al., 2021). The M site contains zinc and magnesium ions stabilizing the enzyme structure and activating a hydroxyl group at the active site to facilitate cGMP hydrolysis while the H-pocket consists of variable hydrophobic residues. L-region in the catalytic domains acts as a lid on the ligand binding domain gating the ligand binding site (Ahmed et al., 2021). All drugs that are currently approved for clinical use exhibit their action by competitive binding to the cGMP binding site in the catalytic domain forming key interactions with residues in Q and H pockets. (Rotella, 2002, Mergia & Stegbauer, 2016).

Combination of *Withania somnifera* (WS), commonly known as ashwagandha or amukkara and *Cardiospermum halicacabum* (CH), commonly known as lesser balloon vine is a commonly used traditional treatment to enhance male virility and to cure erectile dysfunctions. WS is a kind of Indian ginseng, a well-known and frequently used medicinal plant of the Solanaceae family that can be found in the traditional medicine of many countries,

including India and Sri Lanka. (Ven Murthy et al., 2010, Nasimi Doost Azgomi et al., 2018). This herb is believed to promote sexual activity and fertility (Mahdi et al., 2011). However previous studies have failed to establish evidence for its use against erectile dysfunction (Ilayperuma et al., 2002, Mamidi & Thakar, 2011). WS is also an adjuvant in treating different psychosomatic ailments, neuromuscular strength, increasing tissue vitality, and mental and physical endurance. (Mamidi & Thakar, 2011, Ambiyé et al., 2013). Adults tend to benefit from WS extract in regarding sleep (Cheah et al., 2021). Medical plant CH traditionally used to increase male virility while it has a proven potential in increasing sperm count and motile sperm percentage (Peiris et al., 2015). CH is a common annual or perennial climbing plant widely distributed across tropical and subtropical countries. CH is also commonly used in traditional medicine to treat snakebites, rheumatism, and limb stiffness (Kumar et al., 2015) while it has proven antioxidant properties (Sikka et al., 1995).

In the present investigation, Molecular docking and molecular dynamics study was performed in a comparative manner with existing approved PDE5 inhibitors to assess how major compounds from WS and CH would interact with key residues in the catalytic domain of the PDE5 thereby assessing the potential for competitive inhibition of PDE5.

## **2. Materials and Methods**

### ***2.1 Protein preparation for virtual screening***

Following a detailed analysis of existing structures, the PDB ID 1XOZ complex with standard drug tadalafil was selected as the PDE5 target receptor (Oliveira et al., 2019). An additional target validation step was implemented using pathway databases such as KEGG

(**Kanehisa, 2000**) and reactome (**Gillespie et al., 2021**). Any missing side chains in the acquired crystal structure PDB file were inserted using Pdbfixer (**Eastman et al., 2012**), and steric conflicts were resolved (Barnes & Ytreberg, 2019). Water molecules, unwanted ligands, inorganic ions, and organic solvents were eliminated using BIOVIA discovery studio 2022, and hydrogen atoms were added (Ram et al., 2022). The protein was initially decreased energetically in Avogadro (**Hanwell et al., 2012**) using the mmff94 force field, then used for molecular docking virtual screening (Sarkar & Das, 2021). Chimera 1.15 (**Pettersen et al., 2004**) was used to identify the atom types/charges (Faria & Teleschi, 2021). Prepared structure was imported to PyRx software (**Dallakyan & Olson, 2014**) as receptors in the pdbqt format for virtual screening (Hosseini et al., 2020).

## ***2.2 Compound library preparation***

The phytochemical library (See supplementary data) was constructed using 53 major compounds, found in WS and CH and downloaded from the PubChem database (<https://pubchem.ncbi.nlm.nih.gov/>) (**Kim et al., 2022**). After detailed visual validation of structures, Online Smile Translator (OSM) was employed to generate 3D coordinates for phytochemicals (Ferdous et al., 2021). All molecular formats were converted to SDF format using the open babel software (O'Boyle et al., 2011) and was imported into PyRx, where all molecules were minimized using the mmff94 force field in PyRx. All of the phytochemicals were converted to ligands pdbqt format in PyRx.

## ***2.3 Structure-based virtual screening***

The chemical library, which contains 53 ligands, **and 3 controls (tadalafil, sildenafil, and**



**avanafil**) were screened in PyRx by docking with AutoDock Vina against the target protein using the Lamarckian Genetic Algorithm (LGA) (Fuhrmann et al., 2010, Trott & Olson, 2010). Based on available literature and crystal structure information, the virtual screening grid box was constructed to include all binding site residues i.e. Tyr612, His613, Asp654, His657, Gly659, Val660, Ser661, Asn662, Thr723, Asp724, Leu725, Ala726, Asp764, Leu765, Val782, Phe786, Gln789, Leu804, Met805, Gln817 and Phe820. . All polar residues were kept flexible during docking, and exhaustiveness was adjusted to 8. At end of the run, all of the ligands were ranked in order of binding affinity (Quiroga & Villarreal, 2016). All compounds with binding affinities better than or equal to -9.0 kcal/mol were considered as hits while others were eliminated from further studies. Hits were further analyzed for protein-ligand interactions using Protein Ligand Interaction Profiler (<https://plip-tool.biotec.tu-dresden.de/plip-web/plip/index>) (Salentin et al., 2015).

## ***2.4 Interaction analysis***

Hit compounds and three controls were used to binding pose and target ligand interaction analysis using BIOVIA Discovery Studio 2022 (Gogoi et al., 2021). Vina output files were obtained and divided into 10 poses based on their confirmations utilizing “vina split” of autodock tools (Ascone & Sakidja, 2017). The protein target was loaded into Discovery Studio and all poses of ligands and reference drugs having affinity value better than or equal to -9.0 kcal/mol were loaded one at a time. Interaction analysis was done on each confirmation to discover the finest ligand confirmation (Mohankumar et al., 2020).

## ***2.5 Molecular dynamics simulation***

Complexes used for interaction analysis were subjected to for molecular dynamics simulation (MD) analysis. tadalafil, sildenafil and avanafil were served as positive controls for simulation. The MD simulations on docked complexes were done in triplicate using Schrödinger, LLC's Desmond 2020.1 (Bowers, Sacerdoti, et al., 2006). Triplicates were simulated with identical conditions for each MD run to validate the reproducibility of the data. The OPLS-2005 force field (Bowers et al., 2006, Shivakumar et al., 2010) and an explicit solvent model with SPC water molecules were used in this system (Jorgensen et al., 1983). Na<sup>+</sup> and Cl<sup>-</sup> ions were added to neutralize the charge, and a 0.15 M NaCl solution was provided to mimic the physiological environment. TIP3P solvent model (stipulates a trio-site solid water molecule containing charges) was used to solvate docked complexes in an orthorhombic box of 0.5X0.5X0.5 Å<sup>3</sup> size. The NPT ensemble was built using the Nose-Hoover chain coupling technique (Martyna et al., 1994). The production run lasted 100ns with a temperature of 300K , a relaxation period of 1.0ps, and a pressure of 1 bar preserved throughout the simulations (Jukič et al., 2020). A time step of 2fs was used. For pressure control, the Martyna-Tuckerman-Klein chain coupling system (Martyna et al., 1992) barostat method with a relaxation time of 2 ps was used. The particle mesh Ewald approach (Toukmaji et al., 1996) was employed to analyze long-range electrostatic interactions, with the radius for coulomb interactions set at 9. The bonded forces were computed for each trajectory using the RESPA integrator with a time step of 2 fs (Izaguirre et al., 1999). Desmond's simulation interaction analysis tool was used to examine the collected trajectories using multiple MD simulation parameters, including protein root mean square fluctuation (RMSF), root mean square deviation (RMSD), and protein-ligand (PL) interactions.

## ***2.7 ADME-Tox evaluation***

Using the web-server pkCSM (<https://biosig.lab.uq.edu.au/pkcsm/>), and SwissADME (<http://www.swissadme.ch>), the ADME-Tox characteristics (absorption, distribution, metabolism, excretion, and toxicity) of the best hits were analyzed (Pires et al., 2015, Daina et al., 2017). The Structure Data Format (SDF) files of all compounds were used to derive ADMET properties using default values in the servers.

## **3. Results and discussion**

### ***3.1 Molecular docking and molecular dynamics analysis***

#### ***3.1.1 Tadalafil***

Tadalafil, often referred to as Cilais (Coward & Carson, 2008), is a medication used to treat erectile dysfunction and pulmonary hypertension (Minhas et al., 2003, Bethesda, 2012). Several studies conclude that tadalafil has high efficacy and safety as daily dosing (McMahon, 2004, Mirone et al., 2005). Moreover, another study revealed that low-dose consumption may minimize total drug exposure in men who engage in sexual activity more than twice per week and may reduce side effects in men who cannot handle higher PDE5 inhibitor dosages (Costa et al., 2009, Wrishko et al., 2009). In vivo studies have shown the long-term usage safety of tadalafil and its tolerance on the human body (Montorsi et al., 2004, Porst et al., 2006). During one study, tadalafil was well tolerated and safe at dosages of 5, 10, or 20mg administered as necessary up to once daily for 18 to 24 months (Montorsi et al., 2004).

Docking studies were conducted to provide accurate predictions of ligand structure and orientation inside a particular binding site (Meng et al., 2011, Ramírez & Caballero, 2016).

The docking score of Tadalafil with the 1XOZ crystal structure yielded the most significant binding affinity within the list with -12.5 kcal/mol (Table 2). The hydrogen bonding involved

Gln817 which is critical in recognizing its native ligand (Sung et al., 2003, Huai et al., 2004 Zoraghi et al., 2006) as discovered in the 1XOZ structure by re-docking, is a crucial interaction recognized to stabilize the tadalafil. According to previous studies, tadalafil stabilization may also be attributed to residues such as Phe820, Phe786, and Val782 (Huai et al., 2004, Zoraghi et al., 2007). In our research, we identified Phe765, Ala767, Ile768, Val782, Phe786, Leu804, and Phe820 stabilize hydrophobic interactions with Tadalafil. The RMSD values of the protein and ligand during the molecular dynamics simulations were less than 3 Å, indicating that the protein and ligand exhibited relatively stable behavior throughout the simulation (Figure 1A) . The RMSF plot for tadalafil revealed some fluctuations at the catalytic active site interaction at Gln817, with a flexibility range of 0.4 Å to 2.7 Å (Figure 1 C) while the RMSF values along the protein were found below 3 Å, which indicates relative structure rigidity (Li et al., 2010) (Figure 1 B). The hydrogen bond interactions with catalytic residues Gln817 were seen to be retained more than 99% of the simulation time can be observed in the 2D simulation interaction diagram (Figure 1 D) .

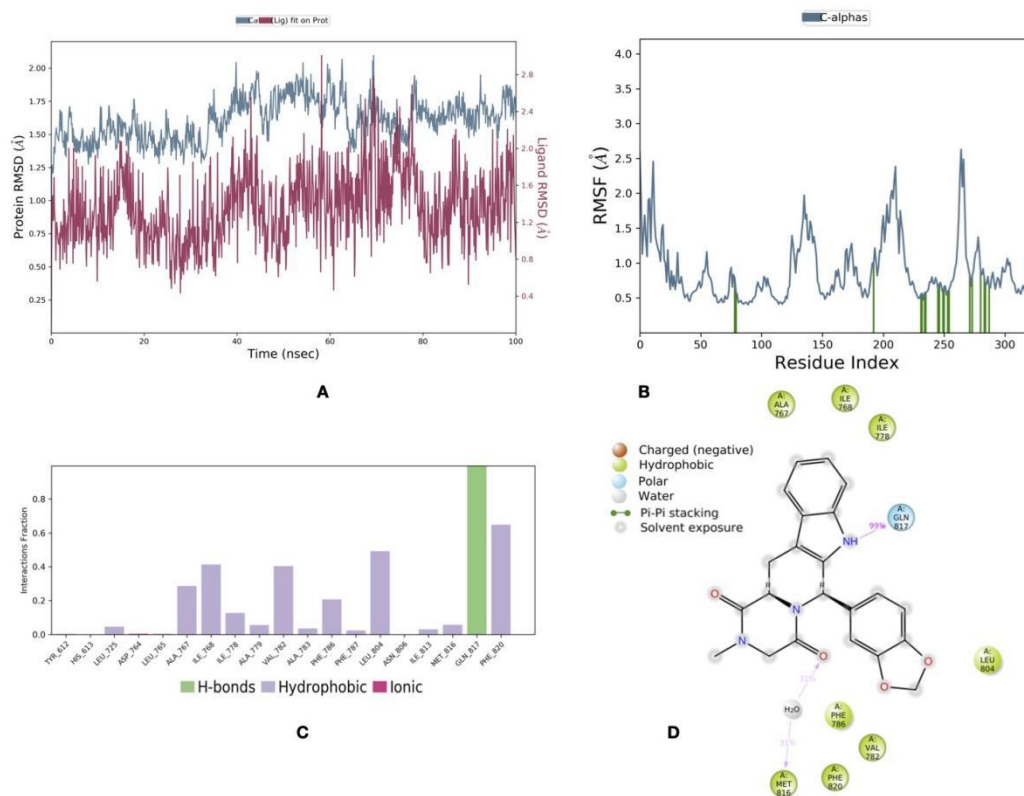


Figure 1. Molecular dynamics simulation analysis on 1XOZ complex with Tadalafil. (A) RMSD fluctuations of protein and ligand during 100 ns simulation runs; (B) Comparative RMSF plot; (C) Histogram showing interaction fractions with active amino acid residues; (D) Schematic representation of ligand indicating percentage interactions with active site residues.

Table 1. Compounds of the *W. somnifera* and *C. halicacabum* and positive controls used for interaction analysis and molecular dynamics simulation.

Compound Tag	Compound name	Pubchem ID	References
--------------	---------------	------------	------------

A1	Withaferin A	265237	(Bethesda, 2012)
A20	Withanolide R	101281364	(H et al., 2022)
A34	17-hydroxy withaferin A	50990201	(Borah et al., 2019)
A37	27-hydroxy withanolide B	15858981	(Borah et al., 2019)
A39	Sitoindoside (IX) or 27-O-glucopyranosyl withaferin A	189586	(Choe et al., 2022)
W26	Apigenin	5280443	(Husain et al., 2022)
W31	Rutin	5280805	(Aati et al., 2022)
C1	Tadalafil	110635	(Frajese et al., 2006)
C2	Avanafil	9869929	(Li et al., 2019)
C3	Sildenafil	135398744	McMurray et al. (2007)

Table 2. Results of molecular docking and interaction analysis. Superscripts indicate the type of interaction ( a- H-bonds; b-hydrophobic interactions; c-salt bridges; d;-halogen bonds e- PI interactions). Gln 817 that form strong H bonds with substrate cGMP is given in bold

Compound Name	Binding energy (kcal/mol)	Interacting Residues
Tadalafil (C1)	-12.5	ALA-767 <sup>b</sup> , ILE-768 <sup>b</sup> , VAL-782 <sup>b</sup> , LEU-804 <sup>b</sup> , MET-816 <sup>b</sup> , <b>GLN-817<sup>ab</sup></b> , PHE-820 <sup>b</sup>
Avanafil (C2)	-9.8	HIS-613 <sup>a</sup> , ASP-764 <sup>a</sup> , GLN-775 <sup>a</sup> , ALA-779 <sup>b</sup> , VAL-782 <sup>b</sup> , MET-816 <sup>b</sup> , <b>GLN-817<sup>ab</sup></b> , PHE-820 <sup>b</sup>
Sildenafil (C3)	-9.6	TYR-612 <sup>a</sup> , ASN-662 <sup>b</sup> , THR-723 <sup>a</sup> , LEU-725 <sup>b</sup> , LEU-765 <sup>b</sup> , LEU-804 <sup>b</sup> , <b>GLN-817<sup>a</sup></b> , PHE-820 <sup>b</sup>
27-hydroxyWitha nolide B (A37)	-11.5	LEU-681 <sup>b</sup> , ALA-779 <sup>a</sup> , VAL-782 <sup>b</sup> , <b>GLN-817<sup>a</sup></b> , PHE-820 <sup>b</sup>
Withaferin A (A1)	-11.5	LEU-681 <sup>b</sup> , THR-723 <sup>a</sup> , LEU-725 <sup>b</sup> , PHE-786 <sup>b</sup> , <b>GLN-817<sup>a</sup></b> , PHE-820 <sup>b</sup>
Sitoindoside ix (A39)	-11.4	TYR-612 <sup>ab</sup> , ASN-662 <sup>a</sup> , GLU-682 <sup>a</sup> , ASP-724 <sup>a</sup> , LEU-725 <sup>a</sup> , ALA-726 <sup>b</sup> , GLN-775 <sup>a</sup> , ILE-778 <sup>b</sup> , VAL-782 <sup>b</sup> , PHE-820 <sup>b</sup>
17-hydroxywithaf erin A (A34)	-11.3	LEU-681 <sup>b</sup> , THR-723 <sup>a</sup> , LEU-725 <sup>b</sup> , PHE-786 <sup>b</sup> , <b>GLN-817<sup>a</sup></b> , PHE-820 <sup>b</sup>
Withanolide R (A20)	-10	HIS-613 <sup>a</sup> , LEU-681 <sup>b</sup> , LEU-804 <sup>b</sup> , MET-816 <sup>b</sup> , <b>GLN-817<sup>b</sup></b> , PHE-820 <sup>b</sup>

Rutin (W31)	-9.6	TYR-612 <sup>a</sup> , ASN-662 <sup>a</sup> , LEU-725 <sup>a</sup> , LEU-726 <sup>a</sup> , ASP-764 <sup>a</sup> , ILE-786 <sup>b</sup> , <b>GLN-817<sup>a</sup></b> , PHE-820 <sup>b</sup>
Apigenin (W26)	-9.2	GLN-775 <sup>a</sup> , ALA-779 <sup>b</sup> , ALA-783 <sup>b</sup> , PHE-786 <sup>b</sup> , LEU-804 <sup>a</sup> , <b>GLN-817<sup>a</sup></b>

### 3.1.2 Avanafil

Avanafil is a PDE5 inhibitor commercially available as Stendra (Kedia et al., 2013). Several studies indicated that avanafil is more selective for PDE5 inhibitors than other PDE inhibitors (Evans & Burke, 2012). This drug is effective as a long-term drug to treat erectile dysfunction (Belkoff et al., 2013). The highest docking score observed for avanafil with the 1XOZ crystal structure was -9.8 kcal/mol (Table 2). During molecular dynamics simulations, the mean RMSD of the protein was less than 3 Å, while the RMSD of the ligand was less than 5 Å, suggesting that the protein and ligand may have shown relatively stable behavior throughout the simulation (Figure 2). However, avanafil initially exhibited variations up to 30 ns of the simulation. However, beyond 30 ns, the compound exhibited no significant RMSD fluctuations (Figure 2 A). Previous in-silico analysis suggested that avanafil stabilizes hydrogen bonds with Tyr612, Ser661, Asp764, and Leu804 and nonpolar bonds with Val782, Phe786, and Gln789 (de Oliveira et al., 2019). According to our study, Tyr612, Asp654, Ile720, Thr723, and Asp764 formed strong hydrogen bonds with avanafil. Moreover, Val782 and Phe786 engaged in hydrophobic interactions. Ionic interactions were also observed in Asp654, Asp724, and Asp764. Since Asp654 and Asp764 have distinct types of bonding (H



bonds and Ionic bonds), overall interaction fractions produced findings that exceeded the interaction fraction score of 1 (Figure 2 C). The RMSF plot for avanafil indicated fluctuations in the catalytic active site interaction at Tyr612, Asp654, Ile720, Thr723, and Asp764, with a flexibility range of 0.4 to 3.5 Å (Figure 2 B). The hydrogen bond interactions with the catalytic residue Asp764 were maintained for more than 88 percent of the simulated duration. Simultaneously, Asp654 retained 87%, Ile720 retained 59%, and Tyr612 retained 58% over the 100 ns can be observed in the 2D simulation interaction diagram (Figure 2 D).

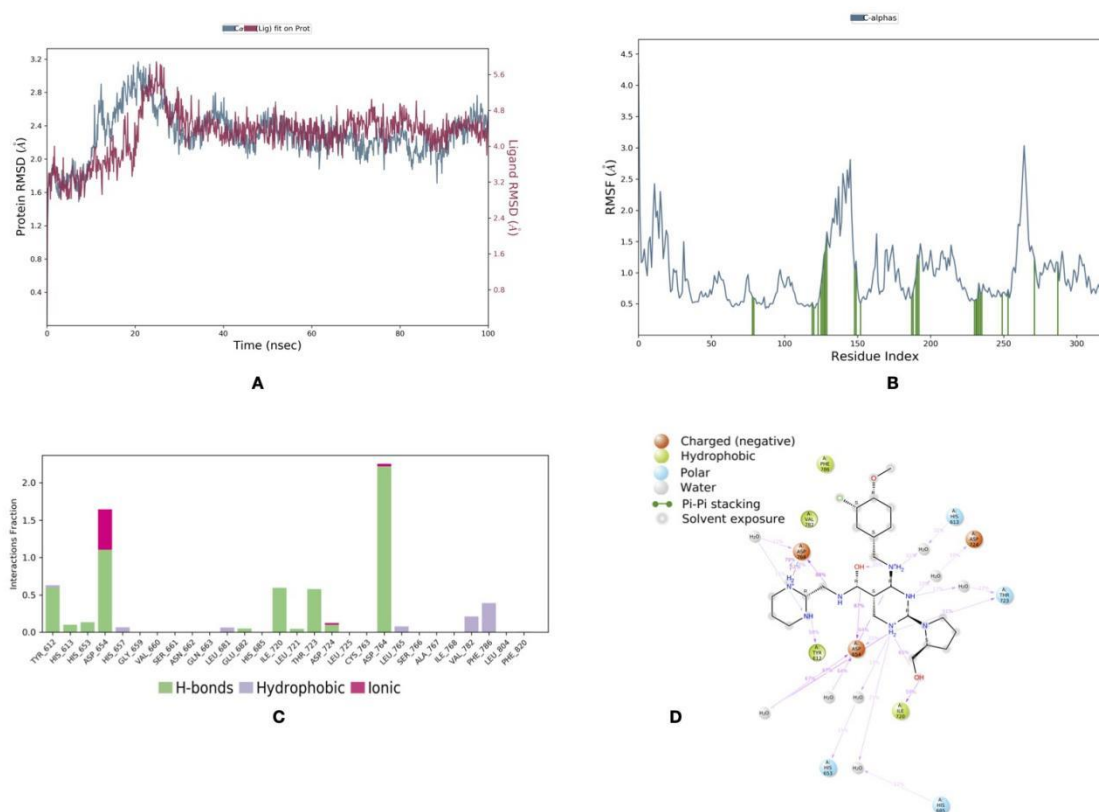


Figure 2. Molecular dynamics simulation analysis on 1XOZ complex with Avanafil. (A) RMSD fluctuations of protein and ligand during 100 ns simulation runs; (B) Comparative RMSF plot; (C) Histogram showing interaction fractions with active amino acid residues; (D) Schematic representation of ligand indicating percentage interactions with active site

residues.

### **3.1.3 Sildenafil**

Sildenafil is a medication prescribed for the treatment of pulmonary arterial hypertension (PAH) and erectile dysfunction (ED) (MedlinePlus, 2019). It is marketed under the Viagra brand and is also offered in generic form (Eardley et al. 2002). Sildenafil works by boosting blood flow to the lungs and penis, resulting in enhanced erections and exercise capacity in patients with PAH (Ramani, 2010). Sildenafil is given orally, up to 30 minutes prior to sexual activity and its effects could last up to 4 hours (Smith & Babos, 2022).

The highest docking score for sildenafil was -9.6 kcal/mol (Table 2). During molecular dynamics simulations, the protein RMSD was less than 2.5Å, while the ligand's RMSD was less than 4.5Å, indicating that the protein and ligand may have exhibited relatively stable behavior throughout the simulation (Figure 3). However, the RMSD plot revealed that Sildenafil fluctuated significantly during the 100ns simulation period (Figure 3 A). Previous in-silico research suggested that sildenafil forms hydrogen bonds with Gln817 and has hydrophobic interactions with Leu765, Ala767, Ile768 and Phe820 (de Oliveira et al., 2019). Gln817 formed strong hydrogen bonds with avanafil, according to our findings. Furthermore, Phe786, Leu804, and Phe820 were involved in hydrophobic interactions. Since Gln817 and Phe820 have multiple bonding sites, overall interaction fractions yielded results that exceeded the interaction fraction score of one (Figure 3 C). With a flexibility range of 0.5 to 3.0, the RMSF plot for sildenafil revealed fluctuations in the catalytic active site interaction at Gln817, Phe786, Leu804, and Phe820 (Figure 3 B). More than 97 percent of the time,

hydrogen bond interactions with the catalytic residue Gln817 were maintained. (Figure 3 D).

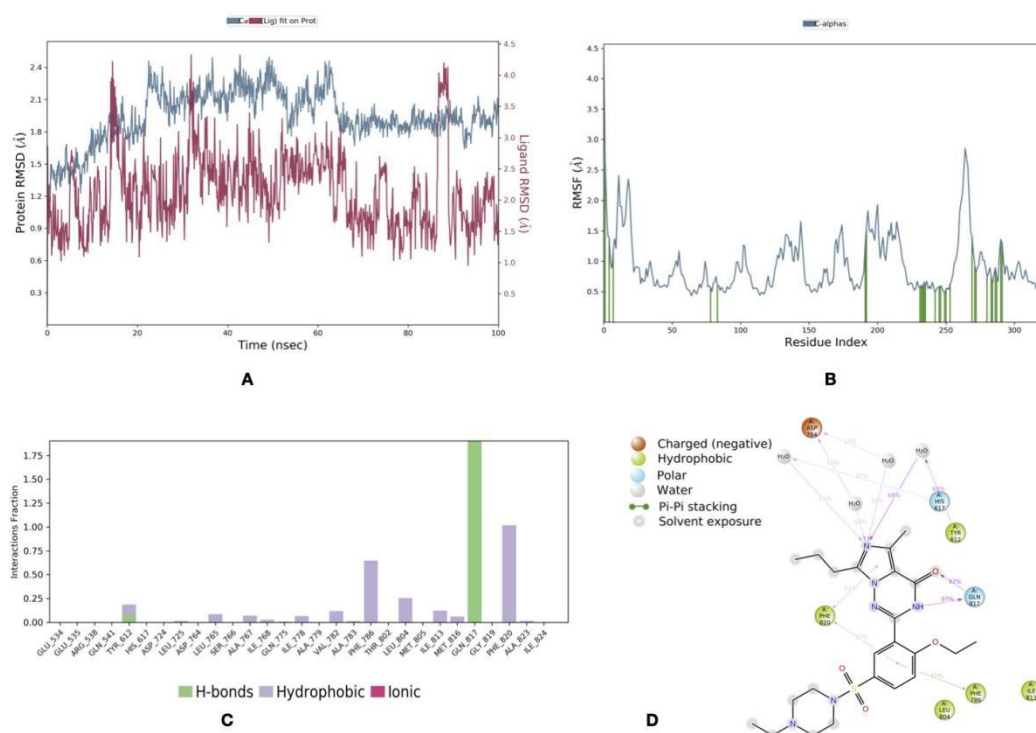


Figure 3. Molecular dynamics simulation analysis on 1XOZ complex with Sildenafil. (A) RMSD fluctuations of protein and ligand during 100 ns simulation runs; (B) Comparative RMSF plot; (C) Histogram showing interaction fractions with active amino acid residues; (D) Schematic representation of ligand indicating percentage interactions with active site residues.

### 3.1.4 27-hydroxywithanolide B

27-hydroxywithanolide B (12-Deoxywithastramonolide) is mainly identified in WS root and leaf (Chaurasiya et al., 2008) and it is recognized as an enzyme inhibitor and an antioxidant (Nile et al., 2019). This compound also shown its potential as a inhibiting the replication of SARS-CoV-2 (Borse et al., 2021). The highest docking score of 27-hydroxywithanolide B

that, when compared to Avanafil and Tadalafil, 27-hydroxywithanolide B is not very stable.

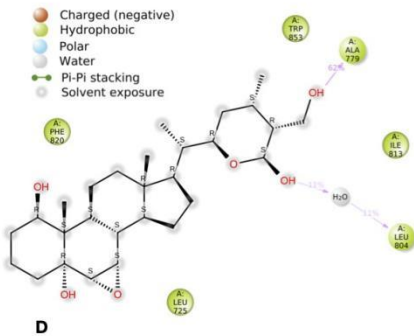


Figure 4. Molecular dynamics simulation analysis on 1XOZ complex with 27-hydroxywithanolide B. (A) RMSD fluctuations of protein and ligand during 100 ns simulation runs; (B) Comparative RMSF plot; (C) Histogram showing interaction fractions with active amino acid residues; (D) Schematic representation of ligand indicating percentage interactions with active site residues.

### 3.1.5 Withaferin A

Withaferin A is the highest bioavailable compound obtained from *W. somnifera* root extracts (Dinesh & Rasool, 2019). This compound is initially recognized for its ability to prevent the growth of cancer cells (Sail & Hadden, 2012). The cytoprotective effect of Withaferin A anticipated the stimulation of the gene-regulating heat shock response factor (Santagata et al., 2011). Several studies have shown that Withaferin A has neuroprotective properties (Dar et al., 2015, Marlow et al., 2017, Zhang et al., 2017, Raziya Banu et al., 2019). It may also act against Parkinson's disease, amyotrophic lateral sclerosis, reactive gliosis, and cerebral infarctions (Jinwal et al., 2021). The highest docking score of Withaferin A with 1XOZ crystal structure was recorded as -11.5 kcal/mol (Table 2). Withaferin A exhibited fluctuations in the first 10 ns of the simulation. After 10 ns, the compound Withaferin A exhibited no substantial RMSD changes compared to the other docked complex trajectories. The protein and ligand RMSD values were nearly superimposed during the overall simulation period and the mean protein RMSD value was lower than 2.0 Å, indicating that the protein and ligand exhibited a steady behavior (Figure 5 A). According to the PL contacts diagram, His653,

His657, Glu682, Ser766, Gln775, and Gln817 contributed significantly to the stabilization of the docked protein-ligand complex (Figure 5 C). Further analysis revealed that, Tyr612, asp724, Leu765, and Val782 show relatively low hydrophobic interactions with the ligand compared to its hydrogen bond interactions.

The RMSF plot for Withaferin A yielded fluctuations at the catalytic active site interaction, His653, His657, Glu682, Ser766, Gln775, and Gln817 with a flexibility range of 0.4 to 2.0 Å (Figure 5 B). The hydrogen bond interactions with the catalytic residue Glu682 were maintained for over 96% of the simulation period. Simultaneously, His653 retained 93%, Gln775 retained 29%, Ser776 retained 26%, and Gln817 retained 11% over the 100 ns period observed in the 2D simulation interaction diagram (Figure 5 D). Furthermore, during modeling, a consistent RMSD behavior of its trajectory was found, confirming the stability of this protein-ligand combination in the active site.

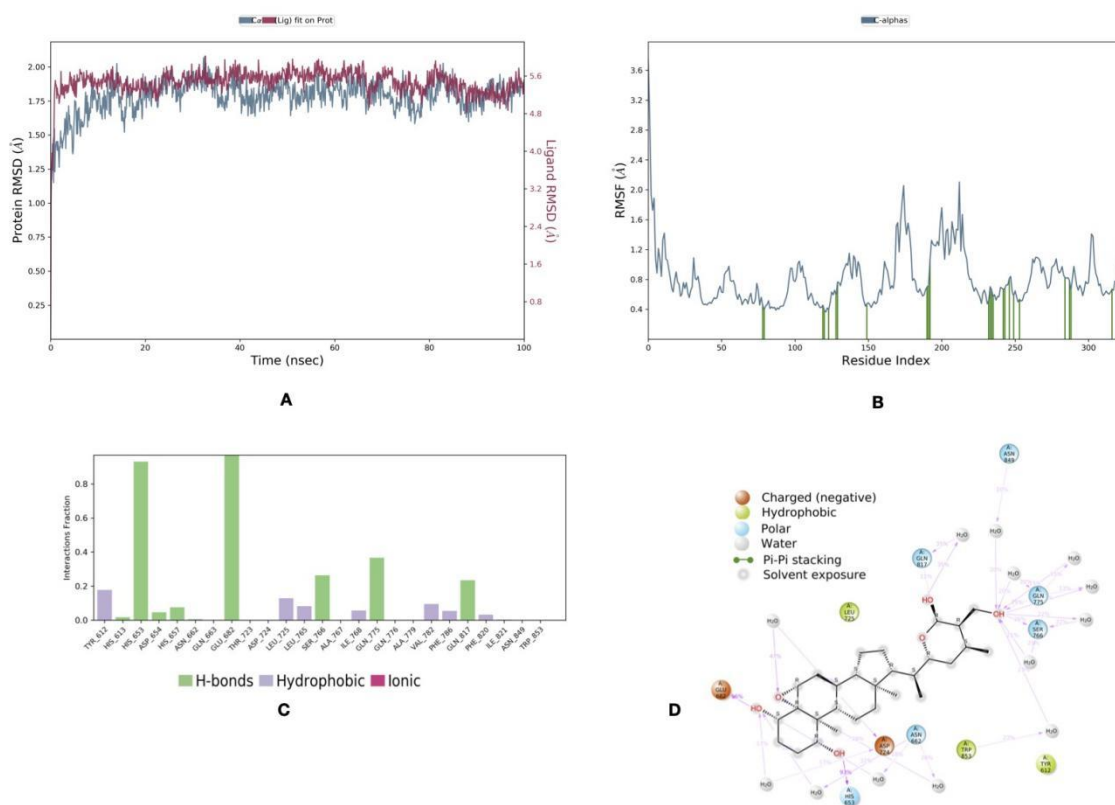


Figure 5. Molecular dynamics simulation analysis on 1XOZ complex with Withaferin A. (A) RMSD fluctuations of protein and ligand during 100 ns simulation runs; (B) Comparative RMSF plot; (C) Histogram showing interaction fractions with active amino acid residues; (D) Schematic representation of ligand indicating percentage interactions with active site residues.

### 3.1.6 Sitaindoside IX

Sitaindoside IX has an antineoplastic activity that is functionally comparable to that of Withaferin A (Jayaprakasam et al., 2003, Zhang et al., 2011). According to research conducted by a group of scientists, this chemical assisted in the formation and maintenance of memory in aged rats (Ghosal et al., 1989). Sitaindoside IX also used as a antistress, anti-Alzheimer's agent (Bokelmann, 2022).

Sitaindoside IX performed a highest docking score of -11.4 kcal/mol with 1XOZ crystal structure (Table 2). Although the PL RMSD chart indicated a lower protein RMSD mean value (2.2 Å), the Ligand RMSD deviates dramatically from 2Å to 14Å throughout the 100ns period (Figure 6 A). The larger ligand RMSD deviation suggests that the protein and ligand exhibited less steady behavior over the simulated period. Sitaindoside IX demonstrated hydrogen bonding interactions with Tyr612, Gln663, Asp724, Gln775, Gln789, and Gln817 based on the PL contacts diagram (Figure 6 C). In addition, Ala545, Leu765, and Phe820 residues formed hydrophobic interactions with Sitaindoside IX. The RMSF plot for Sitaindoside IX yielded the overall less fluctuations at the catalytic active site dyad, Tyr612, Asp724, Gln775, Gln789, and Gln817 with flexibility range of 0.6 to 2.5 Å (Figure 6 B).

The nature of the hydrogen bond contacts with the catalytic pair residues Gln817 was maintained throughout the simulation, which lasted more than 40% of the duration, but the tadalafil interaction on the same residue lasted 99% of the 100ns period. Sitaindoside IX remained stable at 18% with Tyr612, and the interaction between Tyr612 and avanafil lasted 58% throughout the simulation (Figure 6 D). The RMSF chart suggested a steady behavior, while the critical residues were stable.

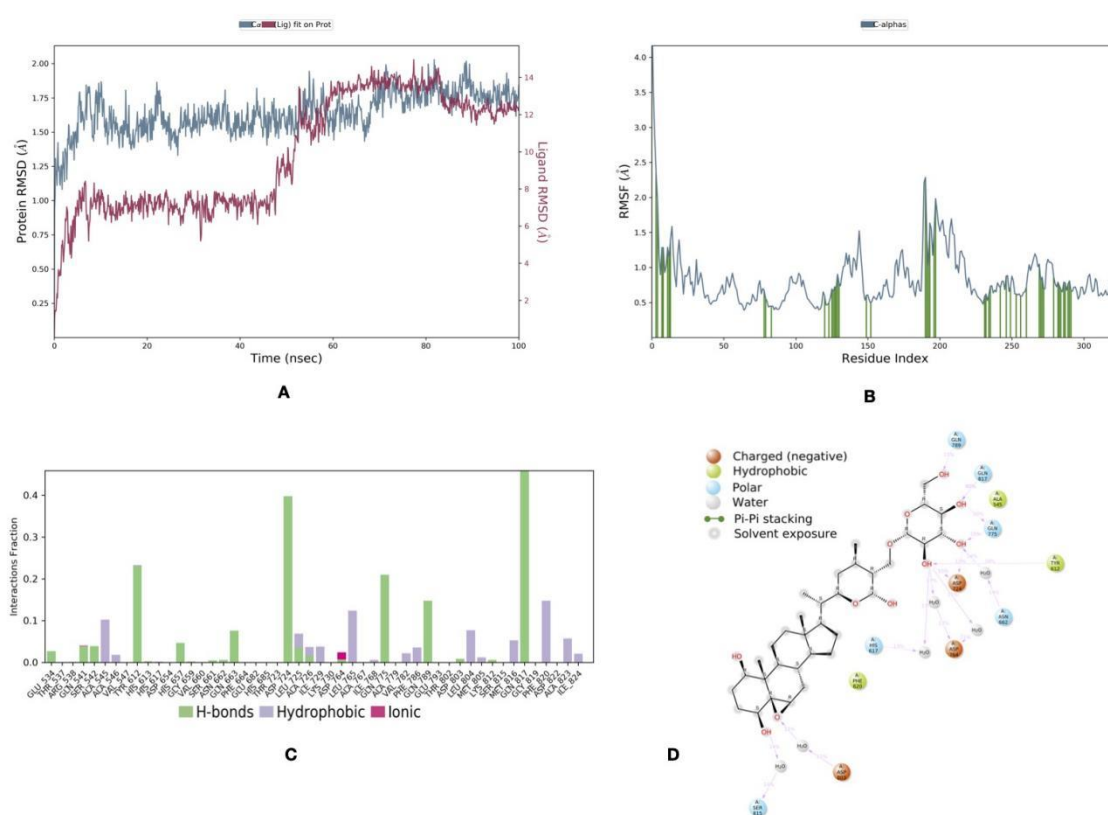


Figure 6. Molecular dynamics simulation analysis on 1XOZ complex with Sitaindoside IX. (A) RMSD fluctuations of protein and ligand during 100 ns simulation runs; (B) Comparative RMSF plot; (C) Histogram showing interaction fractions with active amino acid residues; (D) Schematic representation of ligand indicating percentage interactions with active site residues.



### 3.1.7 17-Hydroxywithaferin A

The docking score validation of 17-Hydroxywithaferin A with 1XOZ crystal structure was recorded as -11.3 kcal/mol (Table 2). The mean protein RMSD was less than 2.2Å, while the mean Ligand RMSD was less than 7Å. The RMSD values of this simulation fluctuated significantly until 60 ns (Figure 7 A). However, again, at 75 ns, there were significant fluctuations. Overall, the figure does not demonstrate steady behavior.

17-Hydroxywithaferin A demonstrated hydrogen bonding interactions with Tyr612, His657, Ser662, Ser662, Ser682, and Gln817 (Figure 7 C). Phe786 and Phe820 further developed hydrophobic interactions with 17-Hydroxywithaferin A. The catalytic active site dyad, Tyr612, His657, Ser662, Ser662, Ser682, and Gln817, exhibited the slightest changes, with a range of flexibility between 0.6 Å and 2 Å, as shown by the RMSF figure (Figure 7 B). The hydrogen bond interactions with the catalytic pair residues His657 were maintained for over 75% of the total simulation duration. In the 2D simulated interaction diagram, Glu682 retained 42%, Asn662 kept 40%, Ser661 retained 24%, Tyr612 retained 15%, and Gln817 retained 12% throughout 100 ns (Figure 7 D). Compared to avanafil and tadalafil, the interaction with the 1XOZ complex exhibited a less stable behavior; still, the essential residues retained significant time over the simulation.

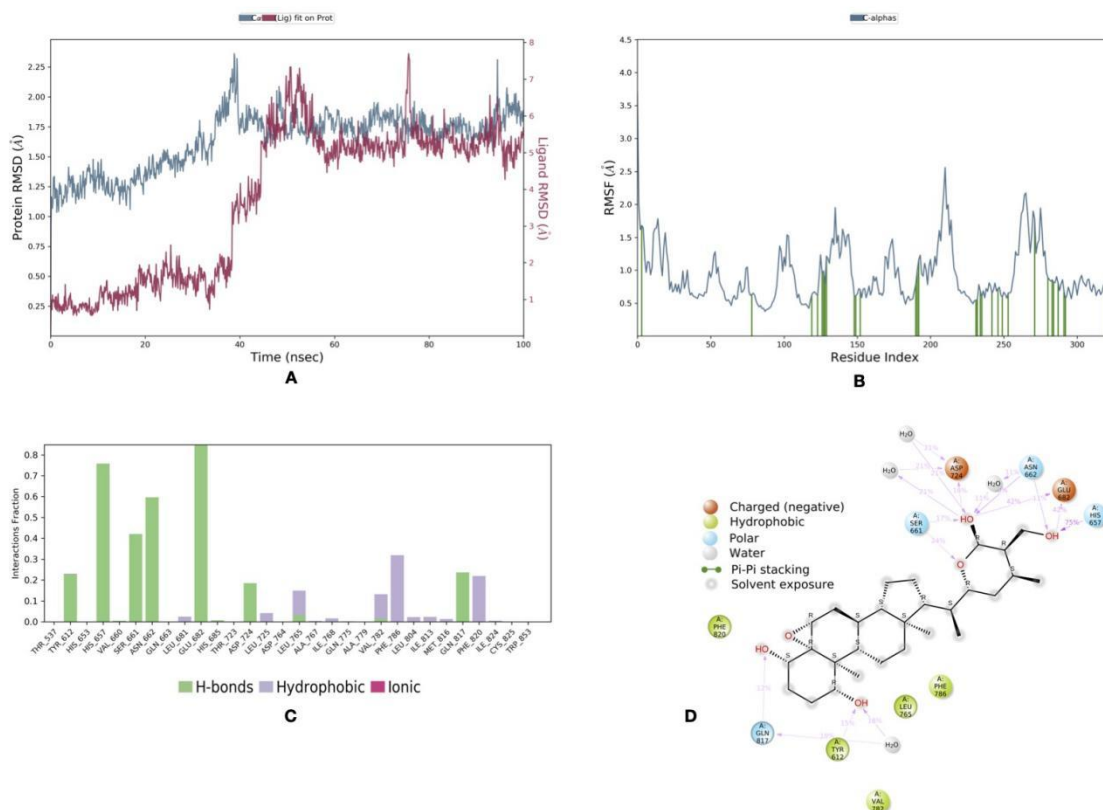


Figure 7. Molecular dynamics simulation analysis on 1XOZ complex with 17-Hydroxywithaferin A. (A) RMSD fluctuations of protein and ligand during 100 ns simulation runs; (B) Comparative RMSF plot; (C) Histogram showing interaction fractions with active amino acid residues; (D) Schematic representation of ligand indicating percentage interactions with active site residues.

### 3.1.8 Withanolide R

The highest docking score of Withanolide R with 1XOZ crystal structure was recorded as -10.0 kcal/mol (Table 2). The RMSD values of these compounds showed significant oscillations until 20 ns, which was true for both the ligand and the protein. The superimposition of the RMSD values for the protein and the ligand indicates stable behavior (Figure 8 A). Withanolide R exhibited weak hydrogen bonding interactions with Thy723,

Thr725, and Leu804. Moreover, hydrogen bonding with Gln817 is very weak. The hydrophobic interactions were performed by Ile729, Val782, Phe786, Leu 804, Phe820, and Ala823 (Figure 8 C). The RMSF plot for Withanolide R yielded the slightest fluctuations at the catalytic active site dyad, Thy723, Gln817, and Thr725, with a flexibility range of 0.5 to 1.5 Å (Figure 8 B) During the simulation, it was discovered that the catalytic pair residues did not sustain any substantial hydrogen bond connections with one another (Figure 8 D). When compared to the tadalafil and avanafil complexes, this ligand complex is considered to have the slightest degree of relevance.

Figure 8. Molecular dynamics simulation analysis on 1XOZ complex with Withanolide R. (A) RMSD fluctuations of protein and ligand during 100 ns simulation runs; (B) Comparative RMSF plot; (C) Histogram showing interaction fractions with active amino acid residues; (D) Schematic representation of ligand indicating percentage interactions with active site

residues.

### *3.1.9 Rutin*

Rutin was discovered to be a natural flavonoid (Chen et al., 2013, Ganeshpurkar & Saluja, 2017) and used in various therapeutic purposes. Rutin demonstrated decreased neuroinflammation in sporadic dementia rat models (Javed et al., 2012). Studies found that rutin has an antidepressant-like effect by increasing noradrenaline and serotonin accessibility in the synaptic cleft (Machado et al., 2008). Rutin improves endothelial function in human endothelial cells by boosting NO production (Ugusman et al., 2014). The fundamental reason for restoring reduced baroreflex sensitivity and 'vascular reactivity' in hypertensive rats is the reduction in oxidative stress generated by rutin when administered orally (Mendes-Junior et al., 2013). In one investigation, rutin was found to have a protective effect against lipid peroxidation-induced damage to human sperm (Moretti et al., 2012). Rutin treatment may help with the several mutilations linked with physical exhaustion (Su et al., 2014).

The highest docking score of rutin with 1XOZ crystal structure was recorded as -9.6 kcal/mol (Table 2). The obtained RMSD values were plotted against the simulation period. The compound rutin demonstrated much-reduced ligand RMSD variations with low angstrom value during the 20-80 ns time frame (Figure 9 A). The mean protein RMSD value was lower than 2.4 Å, and the Ligand RMSD value retained below 3.5 Å suggested that the protein and the ligand went through relatively stable behavior during the simulation. Hydrogen bonding interactions between His612, His613, His617, Ser661, Asn662, Gln663, Leu725, Asp764, Gln775 and Gln817 were discovered (Figure 9 C). The RMSF plot for rutin yielded the slightest fluctuations at the catalytic active site dyad, visualized hydrogen bonding



### 3.1.10 Apigenin

Apigenin was discovered mainly in CH (Chen et al., 2013). Apigenin's therapeutic potential, notably its antioxidant potential and promising function as a neuroprotective drug, in depression, Parkinson's disease, and Alzheimer's disease being investigated (Nabavi et al., 2018). Depending on the dosage, Apigenin may promote muscle relaxation and sleepiness (Shakeri & Boskabady, 2015). According to one research, apigenin is accountable for *T. aphrodisiaca*'s antianxiety function (Kumar & Sharma, 2006).

The obtained RMSD values were displayed against the simulation time for examination after the run. Apigenin demonstrated significant ligand RMSD fluctuations over time. The highest docking score of apigenin with 1XOZ crystal structure was recorded as -9.2 kcal/mol (Table 2). The obtained RMSD data were plotted against the simulation duration for further analysis. The chemical apigenin first showed significant RMSD fluctuations up to 75 ns time scale. The mean protein RMSD value was lower than 2.4 Å, and the Ligand RMSD value below 6.4 Å suggests that the protein and the ligand had reasonably steady deviations throughout the simulation (Figure 10 A). Apigenin interactions exhibited hydrogen bonding with Asp764, Gln775, Ala779, Leu804, and Gln817, as well as hydrophobic interactions with Val782, Phe787, Ile813, Phe820, and Trp853 (Figure 10 C). The RMSF plot for apigenin revealed the slightest changes in the catalytic active site dyads Gln775, and Gln817, with a flexible range of 0.4 to 1.6 (Figure 10 B). Throughout the simulation, which lasted more than 40% of the time, the hydrogen bond interactions with the catalytic pair residues Gln817 were seen to be sustained (Figure 10 D).



(Table 3). However, based on molecular docking and molecular dynamics simulation, the predicted highest potential molecule Withaferin A, stood noticeably between the values of two controls. However, the log P value of Withaferin A is greater than that of the two controls, but this does not break the criteria.

Furthermore, the results revealed that the majority of compounds potentially identified by molecular docking have low TPSA values, implying that their oral bioavailability should be higher than that of the other substances (Table 3) as the oral bioavailability is inversely proportional to TPSA (Freitas, 2006). However, the anticipated molecule Rutin broke the law exhibiting higher H bond donors and acceptors and had a high TPSA value, making it less bioavailable than Tadalafil and Avanafil. The enhanced contemporary medicine, Tadalafil, has a substantially smaller number of hydrogen bond acceptors, molecular weight, and TPSA than many substances in Table, which reportedly adds to its acknowledged benefits over Avanafil. A comprehensive ADME-Tox evaluation can provide a more specific study of pharmacological parameters.

Table 4 shows some parameters for the reference and projected compounds in absorption, distribution, metabolism, excretion, and toxicity. When compared to one another, all compounds had benefits and drawbacks. Specifically analyzing the activity of Withaferin A, there was no discernible change observed in the health consequences or rodent toxicology profiles. Furthermore, the other overall values were marginally lower or higher to those reported with Tadalafil Sildenafil and Avanafil with depicts that Withaferin A may be a promising compound.



Table 3. Results for the calculated Lipinski's rule of five and total polar surface area (TPSA)

Parameter	Tadalafil	Avanafil	Sildenafil	A1	A20	A34	A37	A39	W26	W31
Molecular weight (g/mol)	389.41	483.96	474.587	470.60	470.60	470.60	632.74	270.2	610.52	
logP	2.2113	2.4318	1.6109	3.3513	3.3529	3.3529	1.1771	2.5768	-1.6871	
Number of hydrogen bond acceptors	4	9	8	6	6	6	6	11	5	16
Number of hydrogen bond donors	1	3	1	2	2	2	2	5	3	10
TPSA (Å <sup>2</sup> )	74.88	125.39	121.80	96.36	96.36	96.36	175.51	90.89	269.43	

Table 4. ADME-Tox parameters calculated for the reference and proposed compounds

Parameter	Tadalafil	Avanafil	Sildenafil	A1	A20	A34	A37	A39	W26	W31
GI absorption	High	High	High	High	High	High	High	Low	High	Low

BBB permeant	No	No	No	No	No	No	No	No	No	No
Caco2 permeability	0.946	0.626	0.135	0.885	0.705	0.885	0.792	-0.192	0.917	-0.857
P-glycoprote in substrate	Yes	Yes	Yes	Yes	Yes	Yes	Yes	Yes	Yes	Yes
P-glycoprote in I inhibitor	Yes	Yes	Yes	Yes	Yes	Yes	Yes	Yes	No	No
CNS permeability	-2.212	-3.275	-3.531	-2.416	-2.888	-2.416	-2.589	-3.48	-2.176	-5.578
CYP2D6 substrate	No	No	No	No	No	No	No	No	No	No
CYP3A4 substrate	Yes	No	Yes	Yes	Yes	Yes	Yes	Yes	No	No
CYP1A2 inhibitor	No	No	No	No	No	No	No	No	Yes	No
CYP2C19 inhibitor	Yes	No	No	No	No	No	No	No	No	No
CYP2C9 inhibitor	No	Yes	No	No	No	No	No	No	No	No
CYP2D6 inhibitor	No	No	No	No	No	No	No	No	No	No
CYP3A4 inhibitor	No	Yes	Yes	No	No	No	No	No	Yes	No
AMES toxicity	No	No	No	No	No	No	No	No	No	No
Oral Acute Toxicity (LD50) (mol/kg)	Rat 2.732	2.556	2.655	2.789	2.953	2.789	2.923	3.372	2.327	2.472
Oral Chronic Toxicity (LOAEL) (log mg/kg_bw/day)	Rat 0.915	1.287	1.965	0.956	1.833	0.956	0.864	4.665	1.671	5.706
Skin Sensitisation	No	No	No	No	No	No	No	No	No	No
T.Pyriformis toxicity (log	0.295	0.287	0.286	0.291	0.294	0.291	0.298	0.285	0.458	0.285

## Conclusion

The molecular docking and dynamics modeling technique was used to the natural chemical ingredients of *W. somnifera* and *C. halicacabum* to determine their ability to inhibit the PDE-5 enzyme, which is directly implicated in smooth muscle contraction and relaxation. Among the 53 bioavailable compounds of WS and CS, our research indicated that Withaferin A and Rutin were the most potent natural inhibitors of PDE5. In addition, the RMSD trajectories of Withaferin A and Rutin displayed a very steady behavior with fewer variations than those of other ligands. Stable interactions were observed between the ligand and the catalytic dyad residue Gln 817. With ADMET analysis we observed that Withaferin A is significantly bioavailable than Rutin and it marginally mimics the values of sildenafil, tadalafil and avanafil.

*W. somnifera* and *C. halicacabum* are well-known as antidepressants, sperm count boosters, sleep inducers, antioxidants, and neuroenhancers. This research implies that the Ayurvedic herbs *W. somnifera* and *C. halicacabum* may be an alternative to currently existing PDE5 inhibitors. However, further *in vitro* and *in vivo* testing is required to validate this molecule as a PDE5 inhibitor.

## References

1. Aati, H. Y., Ismail, A., Rateb, M. E., AboulMagd, A. M., Hassan, H. M., & Hetta, M. H. (2022). *Garcinia cambogia* Phenolics as Potent Anti-COVID-19 Agents: Phytochemical

Profiling, Biological Activities, and Molecular Docking. *Plants*, 11(19), 2521.

<https://doi.org/10.3390/plants11192521>

2. Ahmed, W. S., Geethakumari, A. M., & Biswas, K. H. (2021). Phosphodiesterase 5 (PDE5): Structure-function regulation and therapeutic applications of inhibitors. *Biomedicine & Pharmacotherapy*, 134, 111128.  
<https://doi.org/10.1016/j.biopha.2020.111128>
3. Ambiye, V. R., Langade, D., Dongre, S., Aptikar, P., Kulkarni, M., & Dongre, A. (2013). Clinical Evaluation of the Spermatogenic Activity of the Root Extract of Ashwagandha (*Withania somnifera*) in Oligospermic Males: A Pilot Study. *Evidence-Based Complementary and Alternative Medicine*, 2013, 1–6.  
<https://doi.org/10.1155/2013/571420>
4. Andersson, K-E. (2018). PDE5 inhibitors - pharmacology and clinical applications 20 years after sildenafil discovery. *British Journal of Pharmacology*, 175(13), 2554–2565. <https://doi.org/10.1111/bph.14205>
5. Ascone, A., & Sakidja, R. (2017). MDM2 case study: computational protocol utilising protein flexibility and data mining improves ligand binding mode predictions. *International Journal of Computational Biology and Drug Design*, 10(3), 207. <https://doi.org/10.1504/ijcbdd.2017.085402>
6. Barnes, J., & Ytreberg, F. M. (2019). Assessing Foldx for Predicting Protein-Protein Binding Affinity Changes Due to Multiple Mutations. *Biophysical Journal*, 116(3), 336a. <https://doi.org/10.1016/j.bpj.2018.11.1830>

7. Belkoff, L. H., McCullough, A., Goldstein, I., Jones, L., Bowden, C. H., DiDonato, K., Trask, B., & Day, W. W. (2013). An open-label, long-term evaluation of the safety, efficacy and tolerability of avanafil in male patients with mild to severe erectile dysfunction. *International Journal of Clinical Practice*, 67(4), 333–341.  
<https://doi.org/10.1111/ijcp.12065>
8. Bethesda. (2012). LiverTox: Clinical and Research Information on Drug-Induced Liver Injury. In *PubMed*. National Institute of Diabetes and Digestive and Kidney Diseases.  
<https://www.ncbi.nlm.nih.gov/books/NBK547852/>
9. Bischoff, E. (2004). Potency, selectivity, and consequences of nonselectivity of PDE inhibition. *International Journal of Impotence Research*, 16(S1), S11–S14.  
<https://doi.org/10.1038/sj.ijir.3901208>
10. Bokelmann, J. M. (2022, January 1). 26 - *Ashwagandha (Withania somnifera): Root* (J. M. Bokelmann, Ed.). ScienceDirect; Elsevier.  
<https://www.sciencedirect.com/science/article/pii/B978032384676900026X>
11. Borah, K., Sharma, S., & Silla, Y. (2019). Structural bioinformatics-based identification of putative plant based lead compounds for Alzheimer Disease Therapy. *Computational Biology and Chemistry*, 78, 359–366.  
<https://doi.org/10.1016/j.compbiolchem.2018.12.012>
12. Borse, S., Joshi, M., Saggam, A., Bhat, V., Walia, S., Marathe, A., Sagar, S., Chavan-Gautam, P., Girme, A., Hingorani, L., & Tillu, G. (2021). Ayurveda botanicals in COVID-19 management: An in silico multi-target approach. *PLOS ONE*, 16(6), e0248479. <https://doi.org/10.1371/journal.pone.0248479>

13. Bowers, K. J., Chow, D. E., Xu, H., Dror, R. O., Eastwood, M. P., Gregersen, B. A., Klepeis, J. L., Kolossvary, I., Moraes, M. A., Sacerdoti, F. D., Salmon, J. K., Shan, Y., & Shaw, D. E. (2006, November 1). *Scalable Algorithms for Molecular Dynamics Simulations on Commodity Clusters*. IEEE Xplore. <https://doi.org/10.1109/SC.2006.54>
14. Bowers, K. J., Sacerdoti, F. D., Salmon, J. K., Shan, Y., Shaw, D. E., Chow, E., Xu, H., Dror, R. O., Eastwood, M. P., Gregersen, B. A., Klepeis, J. L., Kolossvary, I., & Moraes, M. A. (2006). Molecular dynamics---Scalable algorithms for molecular dynamics simulations on commodity clusters. *Proceedings of the 2006 ACM/IEEE Conference on Supercomputing - SC '06*. <https://doi.org/10.1145/1188455.1188544>
15. Bredt, D. S. (1999). Endogenous nitric oxide synthesis: Biological functions and pathophysiology. *Free Radical Research*, 31(6), 577–596.  
<https://doi.org/10.1080/10715769900301161>
16. Cahill, K. B., Quade, J. H., Carleton, K. L., & Cote, R. H. (2012). Identification of Amino Acid Residues Responsible for the Selectivity of Tadalafil Binding to Two Closely Related Phosphodiesterases, PDE5 and PDE6 \*. *Journal of Biological Chemistry*, 287(49), 41406–41416. <https://doi.org/10.1074/jbc.M112.389189>
17. Chaurasiya, N. D., Uniyal, G. C., Lal, P., Misra, L., Sangwan, N. S., Tuli, R., & Sangwan, R. S. (2008). Analysis of withanolides in root and leaf of *Withania somnifera* by HPLC with photodiode array and evaporative light scattering detection. *Phytochemical Analysis*, 19(2), 148–154. <https://doi.org/10.1002/pca.1029>
18. Cheah, K. L., Norhayati, M. N., Husniati Yaacob, L., & Abdul Rahman, R. (2021). Effect of Ashwagandha (*Withania somnifera*) extract on sleep: A systematic review and

meta-analysis. *PLOS ONE*, 16(9), e0257843.

<https://doi.org/10.1371/journal.pone.0257843>

19. Chen, J., Wei, J.-H., Cai, S.-F., Miao, W.-S., & Pan, L.-W. (2013). [Study on chemical constituents of *Cardiospermum halicacabum*]. *Zhong Yao Cai = Zhongyaocai = Journal of Chinese Medicinal Materials*, 36(2), 228–230.  
<https://pubmed.ncbi.nlm.nih.gov/23901648/>
20. Choe, J., Har Yong, P., & Xiang Ng, Z. (2022). The Efficacy of Traditional Medicinal Plants in Modulating the Main Protease of SARS-CoV-2 and Cytokine Storm. *Chemistry & Biodiversity*, 19(11), e202200655. <https://doi.org/10.1002/cbdv.202200655>
21. Corbin, J. D. (2004). Mechanisms of action of PDE5 inhibition in erectile dysfunction. *International Journal of Impotence Research*, 16(S1), S4–S7.  
<https://doi.org/10.1038/sj.ijir.3901205>
22. Corbin, J. D., Turko, I. V., Beasley, A., & Francis, S. H. (2000). Phosphorylation of phosphodiesterase-5 by cyclic nucleotide-dependent protein kinase alters its catalytic and allosteric cGMP-binding activities. *European Journal of Biochemistry*, 267(9), 2760–2767. <https://doi.org/10.1046/j.1432-1327.2000.01297.x>
23. Costa, P., Grivel, T., & Gehchan Naji. (2009). Tadalafil once daily in the management of erectile dysfunction: patient and partner perspectives. *Patient Preference and Adherence*, 105. <https://doi.org/10.2147/ppa.s3937>
24. Coward, R. M., & Carson, C. C. (2008). Tadalafil in the treatment of erectile dysfunction. *Therapeutics and Clinical Risk Management*, 4(6), 1315–1330.  
<https://www.ncbi.nlm.nih.gov/pmc/articles/PMC2643112/>



25. Daina, A., Michielin, O., & Zoete, V. (2017). SwissADME: a free web tool to evaluate pharmacokinetics, drug-likeness and medicinal chemistry friendliness of small molecules. *Scientific Reports*, 7(1). <https://doi.org/10.1038/srep42717>
26. Dallakyan, S., & Olson, A. J. (2014). Small-Molecule Library Screening by Docking with PyRx. *Methods in Molecular Biology*, 243–250.  
[https://doi.org/10.1007/978-1-4939-2269-7\\_19](https://doi.org/10.1007/978-1-4939-2269-7_19)
27. Dar, N. J., Hamid, A., & Ahmad, M. (2015). Pharmacologic overview of *Withania somnifera*, the Indian Ginseng. *Cellular and Molecular Life Sciences: CMLS*, 72(23), 4445–4460. <https://doi.org/10.1007/s00018-015-2012-1>
28. de Oliveira, I. P., Lescano, C. H., & De Nucci, G. (2019). In Silico Mapping of Essential Residues in the Catalytic Domain of PDE5 Responsible for Stabilization of Its Commercial Inhibitors. *Scientia Pharmaceutica*, 87(4), 29.  
<https://doi.org/10.3390/scipharm87040029>
29. Dhaliwal, A., & Gupta, M. (2020). *PDE5 Inhibitor*. PubMed; StatPearls Publishing.  
<https://www.ncbi.nlm.nih.gov/books/NBK549843/>
30. Dinesh, P., & Rasool, M. (2019, January 1). *Chapter 22 - Herbal Formulations and Their Bioactive Components as Dietary Supplements for Treating Rheumatoid Arthritis* (R. R. Watson & V. R. Preedy, Eds.). ScienceDirect; Academic Press.  
<https://www.sciencedirect.com/science/article/pii/B9780128138205000222>
31. Eardley, I., Ellis, P., Boolell, M., & Wulff, M. (2002). Onset and duration of action of sildenafil for the treatment of erectile dysfunction. *British Journal of Clinical Pharmacology*, 53, 61S65S. <https://doi.org/10.1046/j.0306-5251.2001.00034.x>

32. Eastman, P., Friedrichs, M. S., Chodera, J. D., Radmer, R. J., Bruns, C. M., Ku, J. P., Beauchamp, K. A., Lane, T. J., Wang, L.-P., Shukla, D., Tye, T., Houston, M., Stich, T., Klein, C., Shirts, M. R., & Pande, V. S. (2012). OpenMM 4: A Reusable, Extensible, Hardware Independent Library for High Performance Molecular Simulation. *Journal of Chemical Theory and Computation*, 9(1), 461–469. <https://doi.org/10.1021/ct300857j>
33. Evans, J., & Burke, R. (2012). Avanafil for treatment of erectile dysfunction: review of its potential. *Vascular Health and Risk Management*, 517. <https://doi.org/10.2147/vhrm.s26712>
34. Faria, S. H. D. M., & Teleschi, J. G. (2021). Computational search for drug repurposing to identify potential inhibitors against SARS-COV-2 using Molecular Docking, QTAIM and IQA methods in viral Spike protein – Human ACE2 interface. *Journal of Molecular Structure*, 1232, 130076. <https://doi.org/10.1016/j.molstruc.2021.130076>
35. Ferdous, N., Reza, M. N., Islam, Md. S., Hossain Emon, Md. T., Mohiuddin, A. K. M., & Hossain, M. U. (2021). Newly designed analogues from SARS-CoV inhibitors mimicking the druggable properties against SARS-CoV-2 and its novel variants. *RSC Advances*, 11(50), 31460–31476. <https://doi.org/10.1039/d1ra04107j>
36. Frajese, G. V., Pozzi, F., & Frajese, G. (2006). Tadalafil in the treatment of erectile dysfunction; an overview of the clinical evidence. *Clinical Interventions in Aging*, 1(4), 439–449. <https://doi.org/10.2147/ciia.2006.1.4.439>
37. Freitas, M. P. (2006). MIA-QSAR modelling of anti-HIV-1 activities of some 2-amino-6-arylsulfonylbenzonitriles and their thio and sulfinyl congeners. *Organic & Biomolecular Chemistry*, 4(6), 1154–1159. <https://doi.org/10.1039/B516396J>

38. Fuhrmann, J., Rurainski, A., Lenhof, H.-P., & Neumann, D. (2010). A new Lamarckian genetic algorithm for flexible ligand-receptor docking. *Journal of Computational Chemistry*, NA-NA. <https://doi.org/10.1002/jcc.21478>
39. Ganeshpurkar, A., & Saluja, A. K. (2017). The Pharmacological Potential of Rutin. *Saudi Pharmaceutical Journal*, 25(2), 149–164. <https://doi.org/10.1016/j.jsps.2016.04.025>
40. Ghosal, S., Lal, J., Srivastava, R., Bhattacharya, S. K., Upadhyay, S. N., Jaiswal, A. K., & Chattopadhyay, U. (1989). Immunomodulatory and CNS effects of sitoindosides IX and X, two new glycowithanolides from *Withania somnifera*. *Phytotherapy Research*, 3(5), 201–206. <https://doi.org/10.1002/ptr.2650030510>
41. Gillespie, M., Jassal, B., Stephan, R., Milacic, M., Rothfels, K., Senff-Ribeiro, A., Griss, J., Sevilla, C., Matthews, L., Gong, C., Deng, C., Varusai, T., Ragueneau, E., Haider, Y., May, B., Shamovsky, V., Weiser, J., Brunson, T., Sanati, N., & Beckman, L. (2021). The reactome pathway knowledgebase 2022. *Nucleic Acids Research*, 50(D1), D687–D692. <https://doi.org/10.1093/nar/gkab1028>
42. Gogoi, B., Chowdhury, P., Goswami, N., Gogoi, N., Naiya, T., Chetia, P., Mahanta, S., Chetia, D., Tanti, B., Borah, P., & Handique, P. J. (2021). Identification of potential plant-based inhibitor against viral proteases of SARS-CoV-2 through molecular docking, MM-PBSA binding energy calculations and molecular dynamics simulation. *Molecular Diversity*, 25(3), 1963–1977. <https://doi.org/10.1007/s11030-021-10211-9>

43. Gur, S., Kadowitz, P. J., Serefoglu, E. C., & Hellstrom, W. J. G. (2012). PDE5 Inhibitor Treatment Options for Urologic and Non-Urologic Indications: 2012 Update. *Current Pharmaceutical Design*, 18(34), 5590–5606. <http://www.eurekaselect.com/article/46200>
44. H, S. K., Jade, D., Harrison, M. A., & Sugumar, S. (2022). Identification of natural inhibitor against L1  $\beta$ -lactamase present in *Stenotrophomonas maltophilia*. *Journal of Molecular Modeling*, 28(11), 342. <https://doi.org/10.1007/s00894-022-05336-z>
45. Hanwell, M. D., Curtis, D. E., Lonie, D. C., Vandermeersch, T., Zurek, E., & Hutchison, G. R. (2012). Avogadro: an advanced semantic chemical editor, visualization, and analysis platform. *Journal of Cheminformatics*, 4(1). <https://doi.org/10.1186/1758-2946-4-17>
46. Hosseini, M., Chen, W., & Wang, C. (2020). Computational Molecular Docking and Virtual Screening Revealed Promising SARS-CoV-2 Drugs. *Chemrxiv.org*. <https://doi.org/10.26434/chemrxiv.12237995.v1>
47. Huai, Q., Liu, Y., Francis, S. H., Corbin, J. D., & Ke, H. (2004). Crystal Structures of Phosphodiesterases 4 and 5 in Complex with Inhibitor 3-Isobutyl-1-methylxanthine Suggest a Conformation Determinant of Inhibitor Selectivity. *Journal of Biological Chemistry*, 279(13), 13095–13101. <https://doi.org/10.1074/jbc.m311556200>
48. Husain, I., Ahmad, R., Siddiqui, S., Chandra, A., Misra, A., Srivastava, A., Ahamad, T., Khan, Mohd. F., Siddiqi, Z., Trivedi, A., Upadhyay, S., Gupta, A., Srivastava, A. N., Ahmad, B., Mehrotra, S., Kant, S., Mahdi, A. A., & Mahdi, F. (2022). Structural interactions of phytoconstituent(s) from cinnamon, bay leaf, oregano, and parsley with SARS-CoV -2 nucleocapsid protein: A comparative assessment for development of

potential antiviral nutraceuticals. *Journal of Food Biochemistry*, 46(10).

<https://doi.org/10.1111/jfbc.14262>

49. Ilayperuma, I., Ratnasooriya, W. D., & Weerasooriya, T. R. (2002). Effect of *Withania somnifera* root extract on the sexual behaviour of male rats. *Asian Journal of Andrology*, 4(4), 295–298. <https://pubmed.ncbi.nlm.nih.gov/12508132/>
50. Izaguirre, J. A., Reich, S., & Skeel, R. D. (1999). Longer time steps for molecular dynamics. *The Journal of Chemical Physics*, 110(20), 9853–9864.  
<https://doi.org/10.1063/1.478995>
51. Javed, H., Khan, M. M., Ahmad, A., Vaibhav, K., Ahmad, M. E., Khan, A., Ashafaq, M., Islam, F., Siddiqui, M. S., Safhi, M. M., & Islam, F. (2012). Rutin prevents cognitive impairments by ameliorating oxidative stress and neuroinflammation in rat model of sporadic dementia of Alzheimer type. *Neuroscience*, 210, 340–352.  
<https://doi.org/10.1016/j.neuroscience.2012.02.046>
52. Jayaprakasam, B., Zhang, Y., Seeram, N. P., & Nair, M. G. (2003). Growth inhibition of human tumor cell lines by withanolides from *Withania somnifera* leaves. *Life Sciences*, 74(1), 125–132. <https://doi.org/10.1016/j.lfs.2003.07.007>
53. Jinwal, U., Ram, N., Peak, S., & Perez, A. (2021). Implications of Withaferin A in neurological disorders. *Neural Regeneration Research*, 16(2), 304.  
<https://doi.org/10.4103/1673-5374.290894>
54. Jorgensen, W. L., Chandrasekhar, J., Madura, J. D., Impey, R. W., & Klein, M. L. (1983). Comparison of simple potential functions for simulating liquid water. *The Journal of Chemical Physics*, 79(2), 926–935. <https://doi.org/10.1063/1.445869>

55. Jukič, M., Janežič, D., & Bren, U. (2020). Ensemble Docking Coupled to Linear Interaction Energy Calculations for Identification of Coronavirus Main Protease (3CLpro) Non-Covalent Small-Molecule Inhibitors. *Molecules*, 25(24), 5808.  
<https://doi.org/10.3390/molecules25245808>
56. Kanehisa, M. (2000). KEGG: Kyoto Encyclopedia of Genes and Genomes. *Nucleic Acids Research*, 28(1), 27–30. <https://doi.org/10.1093/nar/28.1.27>
57. Kedia, G. T., Uckert, S., Assadi-Pour, F., Kuczyk, M. A., & Albrecht, K. (2013). Avanafil for the treatment of erectile dysfunction: initial data and clinical key properties. *Therapeutic Advances in Urology*, 5(1), 35–41.  
<https://doi.org/10.1177/1756287212466282>
58. Kim, S., Chen, J., Cheng, T., Gindulyte, A., He, J., He, S., Li, Q., Shoemaker, B. A., Thiessen, P. A., Yu, B., Zaslavsky, L., Zhang, J., & Bolton, E. E. (2022). PubChem 2023 update. *Nucleic Acids Research*. <https://doi.org/10.1093/nar/gkac956>
59. Konstantinos, G., & Petros, P. (2009). Phosphodiesterase-5 inhibitors: future perspectives. *Current Pharmaceutical Design*, 15(30), 3540–3551.  
<https://doi.org/10.2174/138161209789206953>
60. Kumar, E., Mastan, S. K., Sreekanth, N., Chaitanya, G., Reddy, G. A., & Raghunandan, N. (2015). Anti-Arthritic Property of the Ethanolic Leaf Extract of *Cardiospermum Halicacabum* Linn. *Biomedical and Pharmacology Journal*, 1(2), 395–400.  
<https://biomedpharmajournal.org/vol1no2/anti-arthritic-property-of-the-ethanolic-leaf-extract-of-cardiospermum-halicacabum-linn/>

61. Kumar, S., & Sharma, A. (2006). Apigenin: The Anxiolytic Constituent of *Turnera aphrodisiaca*. *Pharmaceutical Biology*, 44(2), 84–90.  
<https://doi.org/10.1080/13880200600591758>
62. Langade, D., Kanchi, S., Salve, J., Debnath, K., & Ambegaokar, D. (2019). Efficacy and Safety of Ashwagandha (*Withania somnifera*) Root Extract in Insomnia and Anxiety: A Double-blind, Randomized, Placebo-controlled Study. *Cureus*, 11(9).  
<https://doi.org/10.7759/cureus.5797>
63. Li, J., Peng, L., Cao, D., He, L., Li, Y., & Wei, Q. (2019). Avanafil for the Treatment of men With Erectile Dysfunction: A Systematic Review and Meta-analysis of Randomized Controlled Trials. *American Journal of Men's Health*, 13(5).  
<https://doi.org/10.1177/1557988319880764>
64. Li, M.-H., Luo, Q., Xue, X.-G., & Li, Z.-S. (2010). Molecular dynamics studies of the 3D structure and planar ligand binding of a quadruplex dimer. *Journal of Molecular Modeling*, 17(3), 515–526. <https://doi.org/10.1007/s00894-010-0746-0>
65. Lipinski, C. A., Lombardo, F., Dominy, B. W., & Feeney, P. J. (2001). Experimental and computational approaches to estimate solubility and permeability in drug discovery and development settings 1PII of original article: S0169-409X(96)00423-1. The article was originally published in *Advanced Drug Delivery Reviews* 23 (1997) 3–25. 1. *Advanced Drug Delivery Reviews*, 46(1-3), 3–26. [https://doi.org/10.1016/s0169-409x\(00\)00129-0](https://doi.org/10.1016/s0169-409x(00)00129-0)
66. Lopresti, A. L., Smith, S. J., Malvi, H., & Kodgule, R. (2019). An investigation into the stress-relieving and pharmacological actions of an ashwagandha (*Withania somnifera*)

extract: A randomized, double-blind, placebo-controlled study. *Medicine*, 98(37), e17186.

<https://doi.org/10.1097/MD.00000000000017186>

67. Machado, D. G., Bettio, L. E. B., Cunha, M. P., Santos, A. R. S., Pizzolatti, M. G., Brighente, I. M. C., & Rodrigues, A. L. S. (2008). Antidepressant-like effect of rutin isolated from the ethanolic extract from *Schinus molle* L. in mice: Evidence for the involvement of the serotonergic and noradrenergic systems. *European Journal of Pharmacology*, 587(1-3), 163–168. <https://doi.org/10.1016/j.ejphar.2008.03.021>
68. Mahdi, A. A., Shukla, K. K., Ahmad, M. K., Rajender, S., Shankhwar, S. N., Singh, V., & Dalela, D. (2011, June 18). *Withania somnifera* Improves Semen Quality in Stress-Related Male Fertility. Evidence-Based Complementary and Alternative Medicine. <https://www.hindawi.com/journals/ecam/2011/576962/>
69. Mamidi, P., & Thakar, A. (2011). Efficacy of Ashwagandha (*Withania somnifera* Dunal. Linn.) in the management of psychogenic erectile dysfunction. *AYU (an International Quarterly Journal of Research in Ayurveda)*, 32(3), 322. <https://doi.org/10.4103/0974-8520.93907>
70. Marlow, M. M., Shah, S. S., Véliz, E. A., Ivan, M. E., & Graham, R. M. (2017). Treatment of adult and pediatric high-grade gliomas with Withaferin A: antitumor mechanisms and future perspectives. *Journal of Natural Medicines*, 71(1), 16–26. <https://doi.org/10.1007/s11418-016-1020-2>
71. Martyna, G. J., Klein, M. L., & Tuckerman, M. (1992). Nosé–Hoover chains: The canonical ensemble via continuous dynamics. *The Journal of Chemical Physics*, 97(4), 2635–2643. <https://doi.org/10.1063/1.463940>



72. Martyna, G. J., Tobias, D. J., & Klein, M. L. (1994). Constant pressure molecular dynamics algorithms. *The Journal of Chemical Physics*, 101(5), 4177–4189.  
<https://doi.org/10.1063/1.467468>
73. McMahon, C. (2004). ED: Efficacy and Safety of Daily Tadalafil in Men with Erectile Dysfunction Previously Unresponsive to On-demand Tadalafil. *The Journal of Sexual Medicine*, 1(3), 292–300. <https://doi.org/10.1111/j.1743-6109.04042.x>
74. McMurray, J. G., Feldman, R. A., Auerbach, S. M., Deriesthal, H., Wilson, N., & Multicenter Study Group. (2007). Long-term safety and effectiveness of sildenafil citrate in men with erectile dysfunction. *Therapeutics and Clinical Risk Management*, 3(6), 975–981. <https://www.ncbi.nlm.nih.gov/pmc/articles/PMC2387281/>
75. MedlinePlus. (2019, October). *Tramadol: MedlinePlus drug information*.  
Medlineplus.gov. <https://medlineplus.gov/druginfo/meds/a695011.html>
76. Mendes-Junior, L. das G., Monteiro, M. M. de O., Carvalho, A. dos S., Queiroz, T. M. de, & Braga, V. de A. (2013). Oral supplementation with the rutin improves cardiovascular baroreflex sensitivity and vascular reactivity in hypertensive rats. *Applied Physiology, Nutrition, and Metabolism*, 38(11), 1099–1106. <https://doi.org/10.1139/apnm-2013-0091>
77. Meng, X.-Y., Zhang, H.-X., Mezei, M., & Cui, M. (2011). Molecular Docking: A Powerful Approach for Structure-Based Drug Discovery. *Current Computer Aided-Drug Design*, 7(2), 146–157. <https://doi.org/10.2174/157340911795677602>
78. Mergia, E., & Stegbauer, J. (2016). Role of Phosphodiesterase 5 and Cyclic GMP in Hypertension. *Current Hypertension Reports*, 18.  
<https://doi.org/10.1007/s11906-016-0646-5>

79. Minhas, S., Kalsi, J., & Ralph, D. (2003). Cialis (tadalafil): a new treatment for erectile dysfunction. *Hospital Medicine*, 64(10), 589–592.  
<https://doi.org/10.12968/hosp.2003.64.10.2323>
80. Mirone, V., Costa, P., Damber, J.-E., Holmes, S., Moncada, I., Van Ahlen, H., Wespes, E., Cordell, W. H., Chan, M., Lembo, D., & Varanese, L. (2005). An evaluation of an alternative dosing regimen with tadalafil, 3 times/week, for men with erectile dysfunction: SURE study in 14 European countries. *European Urology*, 47(6), 846–854; discussion 854. <https://doi.org/10.1016/j.eururo.2005.02.019>
81. Mohankumar, T., Chandramohan, V., Lalithamba, H. S., Jayaraj, R. L., Kumaradhas, P., Sivanandam, M., Hunday, G., Vijayakumar, R., Balakrishnan, R., Manimaran, D., & Elangovan, N. (2020). Design and Molecular dynamic Investigations of 7,8-Dihydroxyflavone Derivatives as Potential Neuroprotective Agents Against Alpha-synuclein. *Scientific Reports*, 10(1), 599.  
<https://doi.org/10.1038/s41598-020-57417-9>
82. Montorsi, F., Verheyden, B., Meuleman, E., Jünemann, K.-P. ., Moncada, I., Valiquette, L., Casabé, A., Pacheco, C., Denne, J., Knight, J., Segal, S., & Watkins, V. S. (2004). Long-term safety and tolerability of tadalafil in the treatment of erectile dysfunction. *European Urology*, 45(3), 339–344; discussion 344-345.  
<https://doi.org/10.1016/j.eururo.2003.11.010>
83. Moretti, E., Mazzi, L., Terzuoli, G., Bonechi, C., Iacoponi, F., Martini, S., Rossi, C., & Collodel, G. (2012). Effect of quercetin, rutin, naringenin and epicatechin on lipid

peroxidation induced in human sperm. *Reproductive Toxicology*, 34(4), 651–657.

<https://doi.org/10.1016/j.reprotox.2012.10.002>

84. Nabavi, S. F., Khan, H., D'onofrio, G., Šamec, D., Shirooie, S., Dehpour, A. R., Argüelles, S., Habtemariam, S., & Sobarzo-Sanchez, E. (2018). Apigenin as neuroprotective agent: Of mice and men. *Pharmacological Research*, 128, 359–365.  
<https://doi.org/10.1016/j.phrs.2017.10.008>
85. Nasimi Doost Azgomi, R., Zomorodi, A., Nazemyieh, H., Fazljou, S. M. B., Sadeghi Bazargani, H., Nejatbakhsh, F., Moini Jazani, A., & Ahmadi AsrBadr, Y. (2018). Effects of *Withania somnifera* on Reproductive System: A Systematic Review of the Available Evidence. *BioMed Research International*, 2018. <https://doi.org/10.1155/2018/4076430>
86. Nile, S. H., Nile, A., Gansukh, E., Baskar, V., & Kai, G. (2019). Subcritical water extraction of withanosides and withanolides from ashwagandha (*Withania somnifera* L) and their biological activities. *Food and Chemical Toxicology*, 132, 110659.  
<https://doi.org/10.1016/j.fct.2019.110659>
87. O'Boyle, N. M., Banck, M., James, C. A., Morley, C., Vandermeersch, T., & Hutchison, G. R. (2011). Open Babel: An open chemical toolbox. *Journal of Cheminformatics*, 3(1).  
<https://doi.org/10.1186/1758-2946-3-33>
88. Peiris, L. D. C., Dhanushka, M. a. T., & Jayathilake, T. a. H. D. G. (2015). Evaluation of Aqueous Leaf Extract of *Cardiospermum halicacabum* (L.) on Fertility of Male Rats. *BioMed Research International*, 2015, e175726.  
<https://doi.org/10.1155/2015/175726>

89. Pettersen, E. F., Goddard, T. D., Huang, C. C., Couch, G. S., Greenblatt, D. M., Meng, E. C., & Ferrin, T. E. (2004). UCSF Chimera--A visualization system for exploratory research and analysis. *Journal of Computational Chemistry*, 25(13), 1605–1612.  
<https://doi.org/10.1002/jcc.20084>
90. Pires, D. E. V., Blundell, T. L., & Ascher, D. B. (2015). pkCSM: Predicting Small-Molecule Pharmacokinetic and Toxicity Properties Using Graph-Based Signatures. *Journal of Medicinal Chemistry*, 58(9), 4066–4072.  
<https://doi.org/10.1021/acs.jmedchem.5b00104>
91. Pole, S. (2006). *Ayurvedic medicine : the principles of traditional practice*. Churchill Livingstone.
92. Porst, H., Giuliano, F., Glina, S., Ralph, D., Casabé, A. R., Elion-Mboussa, A., Shen, W., & Whitaker, J. S. (2006). Evaluation of the Efficacy and Safety of Once-a-Day Dosing of Tadalafil 5mg and 10mg in the Treatment of Erectile Dysfunction: Results of a Multicenter, Randomized, Double-Blind, Placebo-Controlled Trial. *European Urology*, 50(2), 351–359. <https://doi.org/10.1016/j.eururo.2006.02.052>
93. Quiroga, R., & Villarreal, M. A. (2016). Vinardo: A Scoring Function Based on Autodock Vina Improves Scoring, Docking, and Virtual Screening. *PLOS ONE*, 11(5), e0155183. <https://doi.org/10.1371/journal.pone.0155183>
94. Ram, T. S., Munikumar, M., Raju, V. N., Devaraj, P., Boiroju, N. K., Hemalatha, R., Prasad, P. V. V., Gundeti, M., Sisodia, B. S., Pawar, S., Prasad, G. P., Chincholikar, M., Goel, S., Mangal, A., Gaidhani, S., Srikanth, N., & Dhiman, K. S. (2022). In silico evaluation of the compounds of the ayurvedic drug, AYUSH-64, for the action against

- the SARS-CoV-2 main protease. *Journal of Ayurveda and Integrative Medicine*, 13(1), 100413. <https://doi.org/10.1016/j.jaim.2021.02.004>
95. Ramani, G. (2010). Update on the clinical utility of sildenafil in the treatment of pulmonary arterial hypertension. *Drug Design, Development and Therapy*, 61. <https://doi.org/10.2147/dddt.s6208>
  96. Ramírez, D., & Caballero, J. (2016). Is It Reliable to Use Common Molecular Docking Methods for Comparing the Binding Affinities of Enantiomer Pairs for Their Protein Target? *International Journal of Molecular Sciences*, 17(4), 525. <https://doi.org/10.3390/ijms17040525>
  97. Raziya Banu, M., Ibrahim, M., Prabhu, K., & Rajasankar, S. (2019). Ameliorative Effect of Withaferin A on Ageing-Mediated Impairment in the Dopamine System and Its Associated Behavior of Wistar Albino Rat. *Pharmacology*, 103(3-4), 114–119. <https://doi.org/10.1159/000495510>
  98. Rotella, D. P. (2002). Phosphodiesterase 5 inhibitors: current status and potential applications. *Nature Reviews Drug Discovery*, 1(9), 674–682. <https://doi.org/10.1038/nrd893>
  99. Rybalkin, S. D., Yan, C., Bornfeldt, K. E., & Beavo, J. A. (2003). Cyclic GMP Phosphodiesterases and Regulation of Smooth Muscle Function. *Circulation Research*, 93(4), 280–291. <https://doi.org/10.1161/01.res.0000087541.15600.2b>
  100. Sail, V., & Hadden, M. K. (2012, January 1). *Chapter Eighteen - Notch Pathway Modulators as Anticancer Chemotherapeutics* (M. C. Desai, Ed.). ScienceDirect;

Academic Press.

<https://www.sciencedirect.com/science/article/abs/pii/B9780123964922000187>

101. Salentin, S., Schreiber, S., Haupt, V. J., Adasme, M. F., & Schroeder, M. (2015). PLIP: fully automated protein–ligand interaction profiler. *Nucleic Acids Research*, 43(W1), W443–W447. <https://doi.org/10.1093/nar/gkv315>
102. Salve, J., Pate, S., Debnath, K., & Langade, D. (2019). Adaptogenic and Anxiolytic Effects of Ashwagandha Root Extract in Healthy Adults: A Double-blind, Randomized, Placebo-controlled Clinical Study. *Cureus*, 11(12). <https://doi.org/10.7759/cureus.6466>
103. Santagata, S., Xu, Y., Wijeratne, E. M. K., Kontnik, R., Rooney, C., Perley, C. C., Kwon, H., Clardy, J., Kesari, S., Whitesell, L., Lindquist, S., & Gunatilaka, A. A. L. (2011). Using the Heat-Shock Response To Discover Anticancer Compounds that Target Protein Homeostasis. *ACS Chemical Biology*, 7(2), 340–349. <https://doi.org/10.1021/cb200353m>
104. Sarkar, K., & Das, R. K. (2021). Preliminary Identification of Hamamelitannin and Rosmarinic Acid as COVID-19 Inhibitors Based on Molecular Docking. *Letters in Drug Design & Discovery*, 18(1), 67–75. <https://doi.org/10.2174/1570180817999200802032126>
105. Shakeri, F., & Boskabady, M. H. (2015). A review of the relaxant effect of various medicinal plants on tracheal smooth muscle, their possible mechanism(s) and potency. *Journal of Ethnopharmacology*, 175, 528–548. <https://doi.org/10.1016/j.jep.2015.10.017>

106. Shivakumar, D., Williams, J., Wu, Y., Damm, W., Shelley, J., & Sherman, W. (2010). Prediction of Absolute Solvation Free Energies using Molecular Dynamics Free Energy Perturbation and the OPLS Force Field. *Journal of Chemical Theory and Computation*, 6(5), 1509–1519. <https://doi.org/10.1021/ct900587b>
107. Siddique, A. A., Joshi, P., Misra, L., Sangwan, N. S., & Darokar, M. P. (2014). 5,6-de-epoxy-5-en-7-one-17-hydroxy withaferin A, a new cytotoxic steroid from *Withania somnifera* L. Dunal leaves. *Natural Product Research*, 28(6), 392–398. <https://doi.org/10.1080/14786419.2013.871545>
108. Sikka, S. C., Rajasekaran, M., & Hellstrom, W. J. (1995). Role of oxidative stress and antioxidants in male infertility. *Journal of Andrology*, 16(6), 464–468. <https://pubmed.ncbi.nlm.nih.gov/8867595/>
109. *Sildenafil (Oral Route) Proper Use - Mayo Clinic*. (n.d.). [www.mayoclinic.org](http://www.mayoclinic.org). <https://www.mayoclinic.org/drugs-supplements/sildenafil-oral-route/proper-use/drg-20066989>
110. Smith, B. P., & Babos, M. (2022). *Sildenafil*. PubMed; StatPearls Publishing. <https://pubmed.ncbi.nlm.nih.gov/32644404/>
111. Socała, K., Nieoczym, D., Pieróg, M., Szuster-Ciesielska, A., Wyska, E., & Wlaź, P. (2016). Antidepressant-like activity of sildenafil following acute and subchronic treatment in the forced swim test in mice: effects of restraint stress and monoamine depletion. *Metabolic Brain Disease*, 31(5), 1095–1104. <https://doi.org/10.1007/s11011-016-9852-8>

112. Soderling, S. H., & Beavo, J. A. (2000). Regulation of cAMP and cGMP signaling: new phosphodiesterases and new functions. *Current Opinion in Cell Biology*, 12(2), 174–179. [https://doi.org/10.1016/s0955-0674\(99\)00073-3](https://doi.org/10.1016/s0955-0674(99)00073-3)
113. Su, K.-Y., Yu, C. Y., Chen, Y.-W., Huang, Y.-T., Chen, C.-T., Wu, H.-F., & Chen, Y.-L. S. (2014). Rutin, a Flavonoid and Principal Component of *Saussurea Involucrata*, Attenuates Physical Fatigue in a Forced Swimming Mouse Model. *International Journal of Medical Sciences*, 11(5), 528–537. <https://doi.org/10.7150/ijms.8220>
114. Sung, B.-J., Yeon Hwang, K., Ho Jeon, Y., Lee, J. I., Heo, Y.-S., Hwan Kim, J., Moon, J., Min Yoon, J., Hyun, Y.-L., Kim, E., Jin Eum, S., Park, S.-Y., Lee, J.-O., Gyu Lee, T., Ro, S., & Myung Cho, J. (2003). Structure of the catalytic domain of human phosphodiesterase 5 with bound drug molecules. *Nature*, 425(6953), 98–102. <https://doi.org/10.1038/nature01914>
115. Toukmaji, A. Y., & Board, J. A. (1996). Ewald summation techniques in perspective: a survey. *Computer Physics Communications*, 95(2-3), 73–92. [https://doi.org/10.1016/0010-4655\(96\)00016-1](https://doi.org/10.1016/0010-4655(96)00016-1)
116. Trott, O., & Olson, A. J. (2009). AutoDock Vina: Improving the speed and accuracy of docking with a new scoring function, efficient optimization, and multithreading. *Journal of Computational Chemistry*, 31(2), NA-NA. <https://doi.org/10.1002/jcc.21334>
117. Tsai, E. J., & Kass, D. A. (2009). Cyclic GMP signaling in cardiovascular pathophysiology and therapeutics. *Pharmacology & Therapeutics*, 122(3), 216–238. <https://doi.org/10.1016/j.pharmthera.2009.02.009>



118. Turko, I. V., Ballard, S. A., Francis, S. H., & Corbin, J. D. (1999). Inhibition of cyclic GMP-binding cyclic GMP-specific phosphodiesterase (Type 5) by sildenafil and related compounds. *Molecular Pharmacology*, 56(1), 124–130.  
<https://doi.org/10.1124/mol.56.1.124>
119. TURKO, V. I., FRANCIS, H. S., & CORBIN, D. J. (1998). Binding of cGMP to both allosteric sites of cGMP-binding cGMP-specific phosphodiesterase (PDE5) is required for its phosphorylation. *Biochemical Journal*, 329(3), 505–510.  
<https://doi.org/10.1042/bj3290505>
120. Ugusman, A., Zakaria, Z., Chua, K. H., Megat Mohd Nordin, N. A., & Abdullah Mahdy, Z. (2014). Role of Rutin on Nitric Oxide Synthesis in Human Umbilical Vein Endothelial Cells. *The Scientific World Journal*, 2014, 1–9.  
<https://doi.org/10.1155/2014/169370>
121. Ven Murthy, M. R., Ranjekar, P. K., Ramassamy, C., & Deshpande, M. (2010). Scientific basis for the use of Indian ayurvedic medicinal plants in the treatment of neurodegenerative disorders: ashwagandha. *Central Nervous System Agents in Medicinal Chemistry*, 10(3), 238–246. <https://doi.org/10.2174/1871524911006030238>
122. Wal, P., & Wal, A. (2013, January 1). *Chapter 34 - An Overview of Adaptogens with a Special Emphasis on Withania and Rhodiola* (D. Bagchi, S. Nair, & C. K. Sen, Eds.). ScienceDirect; Academic Press.  
<https://www.sciencedirect.com/science/article/pii/B9780123964540000345>
123. Wrishko, R., Sorsaburu, S., Wong, D., Strawbridge, A., & McGill, J. (2009). Safety, efficacy, and pharmacokinetic overview of low-dose daily administration of

tadalafil. *The Journal of Sexual Medicine*, 6(7), 2039–2048.

<https://doi.org/10.1111/j.1743-6109.2009.01301.x>

124. Yadav, A. K., & Singh, T. R. (2021). Novel inhibitors design through structural investigations and simulation studies for human PKMTs (SMYD2) involved in cancer. *Molecular Simulation*, 47(14), 1149–1158.
- <https://doi.org/10.1080/08927022.2021.1957882>
125. Zhang, H., Samadi, A. K., Gallagher, R. J., Araya, J. J., Tong, X., Day, V. W., Cohen, M. S., Kindscher, K., Gollapudi, R., & Timmermann, B. N. (2011). Cytotoxic withanolide constituents of *Physalis longifolia*. *Journal of Natural Products*, 74(12), 2532–2544. <https://doi.org/10.1021/np200635r>
126. Zhang, Q.-Z., Guo, Y.-D., Li, H.-M., Wang, R.-Z., Guo, S.-G., & Du, Y.-F. (2017). Protection against cerebral infarction by Withaferin A involves inhibition of neuronal apoptosis, activation of PI3K/Akt signaling pathway, and reduced intimal hyperplasia via inhibition of VSMC migration and matrix metalloproteinases. *Advances in Medical Sciences*, 62(1), 186–192. <https://doi.org/10.1016/j.advms.2016.09.003>
127. Zhu, B., & Strada, S. (2007). The Novel Functions of cGMP-Specific Phosphodiesterase 5 and its Inhibitors in Carcinoma Cells and Pulmonary/Cardiovascular Vessels. *Current Topics in Medicinal Chemistry*, 7(4), 437–454.
- <https://doi.org/10.2174/156802607779941198>
128. Zoraghi, R., Corbin, J. D., & Francis, S. H. (2006). Phosphodiesterase-5 Gln817 Is Critical for cGMP, Vardenafil, or Sildenafil Affinity. *Journal of Biological Chemistry*, 281(9), 5553–5558. <https://doi.org/10.1074/jbc.m510372200>

129. Zoraghi, R., Francis, S. H., & Corbin, J. D. (2007). Critical amino acids in phosphodiesterase-5 catalytic site that provide for high-affinity interaction with cyclic guanosine monophosphate and inhibitors. *Biochemistry*, 46(47), 13554–13563.  
<https://doi.org/10.1021/bi7010702>